



Review of advanced sensor devices employing nanoarchitectonics concepts

Katsuhiko Ariga^{*1,2}, Tatsuyuki Makita², Masato Ito², Taizo Mori^{1,2}, Shun Watanabe² and Jun Takeya^{1,2}

Review

[Open Access](#)

Address:

¹WPI-MANA, National Institute for Materials Science, 1-1 Namiki, Tsukuba 305-0044, Japan and ²Department of Advanced Materials Science, Graduate School of Frontier Sciences, The University of Tokyo, 5-1-5 Kashiwanoha, Kashiwa 277-8561, Japan

Email:

Katsuhiko Ariga^{*} - ARIGA.Katsuhiko@nims.go.jp

^{*} Corresponding author

Keywords:

interface; molecular recognition; nanoarchitectonics; sensor; thin film

Beilstein J. Nanotechnol. **2019**, *10*, 2014–2030.

doi:10.3762/bjnano.10.198

Received: 15 June 2019

Accepted: 06 September 2019

Published: 16 October 2019

This article is part of the thematic issue "Nanoarchitectonics: bottom-up creation of functional materials and systems".

Associate Editor: N. Motta

© 2019 Ariga et al.; licensee Beilstein-Institut.

License and terms: see end of document.

Abstract

Many recent advances in sensor technology have been possible due to nanotechnological advancements together with contributions from other research fields. Such interdisciplinary collaborations fit well with the emerging concept of nanoarchitectonics, which is a novel conceptual methodology to engineer functional materials and systems from nanoscale units through the fusion of nanotechnology with other research fields, including organic chemistry, supramolecular chemistry, materials science and biology. In this review article, we discuss recent advancements in sensor devices and sensor materials that take advantage of advanced nanoarchitectonics concepts for improved performance. In the first part, recent progress on sensor systems are roughly classified according to the sensor targets, such as chemical substances, physical conditions, and biological phenomena. In the following sections, advancements in various nanoarchitectonic motifs, including nanoporous structures, ultrathin films, and interfacial effects for improved sensor function are discussed to realize the importance of nanoarchitectonic structures. Many of these examples show that advancements in sensor technology are no longer limited by progress in microfabrication and nanofabrication of device structures – opening a new avenue for highly engineered, high performing sensor systems through the application of nanoarchitectonics concepts.

Review

Introduction

Detection systems for various chemical, physical, environmental, and biological targets, so-called sensors, have been continuously explored [1-4]. Although their usefulness was recognized even in the early stages of modern science and technolo-

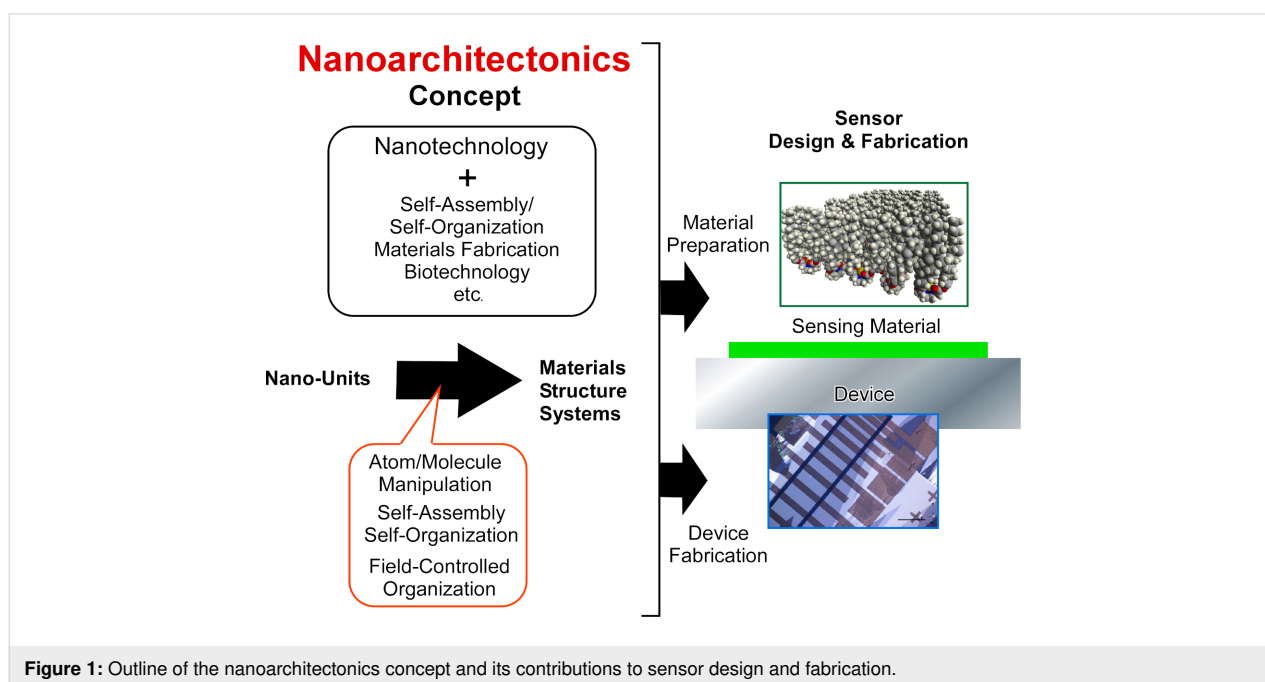
gy, the importance of sensors has been recently re-evaluated in the context of current research developments. Today, sensors play an important role in technological advancement for various social demands. There are currently many strategies being

pursued for the production of functional materials [5-8], the detection of various risks [9-11], environmental remediation including pollution problems [12-14], energy production [15-17], energy and electricity storage [18-20], device technologies [21-23], and biomedical treatment [24-27], and the targets must be detected with high selectivity, high efficiency, environmental friendliness, and with low cost and low emission. Various fundamental areas of science and technology, such as organic synthesis [28-30], supramolecular organization [31-35], physical fabrication [36-38] and biotechnology [39-41], are expected to solve these problems where some additional factors have to be considered in order to achieve a high degree of control over the structure. This is accomplished by two major processes: (i) selective and sensitive recognition of external inputs (stimuli, substrates, etc.) and (ii) efficient logical conversion to outputs (response, energy, products, etc.). Good sensing systems have many contributions regarding the former part. This is why the importance of sensors has been re-recognized in modern sensor technology.

In recent decades, the development of sensor technologies has highly depended on advancements in microfabrication and nanofabrication of device structures. These so-called nanotechnological advancements enable us to prepare sensing devices with various advantageous features with an ultrasmall device size (thus requiring an ultrasmall amount of the target sample), highly integrated connection, and high sensitivity [42,43]. In addition to these nanotechnological advancements in device fabrication, sensing materials for molecular recognition have been continuously explored on the basis of supramolecular

chemistry with the aid of synthetic organic chemistry and materials science [44-46]. Therefore, further developments in sensors can be made by the combined efforts in nanotechnology and other research fields including supramolecular chemistry, organic synthesis, and materials sciences. In case of biosensors, contributions from biology play important roles [47-50]. These cross disciplinary collaborations that are necessary for sensor development fit well with the emerging concept of nanoarchitectonics [51,52], which involves a paradigm shift in research efforts to engineer functional materials and systems from nanoscale units through the fusion of nanotechnology with other research fields, including organic chemistry, supramolecular chemistry, materials science and biology. It can thus be said that the future developments of sensors can be supported by the field of nanoarchitectonics [53] (Figure 1).

The nanoarchitectonics concept was originally proposed by Masakazu Aono [54,55]. This conceptual methodology corresponds to the creation of functional materials from nanoscale units through combined processes, including organic synthesis, atomic/molecular manipulation, self-assembly, self-organization, stimuli-based arrangement, and biological treatment, depending on their necessity [56,57]. The high generality of the nanoarchitectonics concept can be applied to a wide range of research concepts, such as materials production [58-60], structure facilitation [61-65], catalysis [66,67], energy technology [68,69], environmental problems [70,71], biological investigation [72-75], and biomedical applications [76-78]. As compared with simple self-assembly processes, nanoarchitectonics is advantageous for architecting hierarchical structures and



interfacing between materials and devices. In addition, the fabrication of sensor structures is one of the main outputs of nanoarchitectonics [79,80].

The nanoarchitectonics concept should also include uncertainties related to phenomena that occur on the nanoscale, where thermal and statistical fluctuations as well as quantum effects cannot be avoided [81]. The properties and functions on the nanoscale often result from the harmonization of various interactions. This feature is also found in many biological systems in which functional molecules harmonize under unavoidable thermal fluctuations. The nanoarchitectonics approach and biological processes thus share many of the same features [82]. Therefore, the design and fabrication of biosensors based on the nanoarchitectonics concept may have many particular advantages.

In this review article, we first discuss several examples of recent progress in sensor systems whose advanced nanoarchitectonic design and fabrication allowed for better performance. The examples are roughly classified according to the sensor target, such as chemical substances, physical conditions, and biological phenomena. In the following sections, advancements employing nanoarchitectonic motifs, including nanoporous structures, ultrathin films, and interfacial effects for sensor functions, are discussed. Based on these descriptions, we hope that we can impress the importance upon the advancements of sensor functions with nanoscale control, and especially the importance of nanoarchitectonics in the improvement of these concepts.

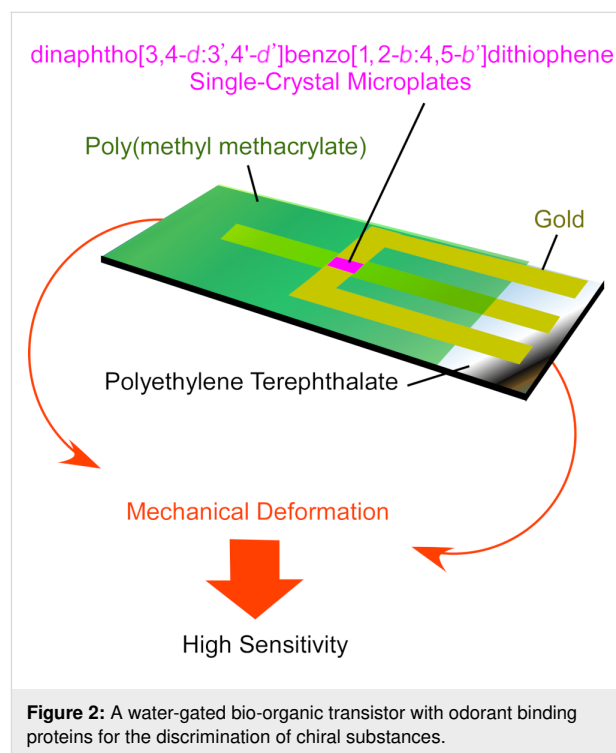
Recent examples of advanced sensors

Advancements in sensor capabilities, including sensitivity, selectivity and usability, can be accomplished by ultrafine design of device mechanisms and sensing material structures. Both the device and sensing material design can be accomplished with a combined concept, nanoarchitectonics, derived from nanotechnology (mainly for the device) and supramolecular chemistry and others (mainly for the sensing materials). For example, Osica recently reported sensor systems for selective acetone vapor detection [83,84]. The prepared systems are supported by two separate innovations, a membrane-type surface stress sensor as a novel nanomechanical device and a highly networked capsular nanoarchitecture of silica–porphyrin hybrid as the sensing material. Not limited to this particular case, innovations from both the device side and the materials side for improved sensors has been continuously pursued.

Sensors for chemical substances

Mainly due to the high demand to solve environmental problems, vapor sensors and gas-phase chemical sensors have been

actively researched. Tang and co-workers accomplished drastic improvement of sensitivity of H₂S gas detection by mechanical deformation of ultrathin single crystals of dinaphtho[3,4-*d*:3',4'-*d'*]benzo[1,2-*b*:4,5-*b'*]dithiophene in organic field effect transistors [85] (Figure 2). At the tensile state of the crystals, the sensitivity to H₂S gas at 1 ppm increased by 400% as compared to the original unstressed state. Upon exposure of the sensor crystals to H₂S gas, the adsorbed H₂S gas molecules induce a current between the source and drain. Changes in the intermolecular packing of the sensing organic crystals may cause more exposure of active sites to H₂S gas and dramatic shifts of mobility, resulting in unexpectedly high sensitivity. This example indicates that the delicate modulation of nanoarchitectures can improve chemical sensor capabilities.



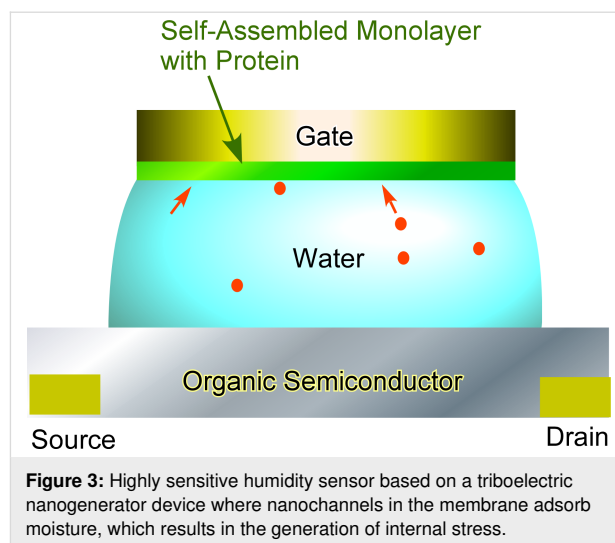
As an example of nanoarchitectonics effects between multiple components in sensing materials, Chen, Shi, and co-workers demonstrated highly sensitive resistance-based NO_x gas sensors incorporating a dispersed composite of Co₃O₄ nanoparticles in black phosphorous thin films [86]. The composite structures were engineered by functionalization of black phosphorous nanosheets with branched polyethylenimine to which Co₃O₄ nanoparticles were included with a hydrothermal process. The sensor composite structures showed ultrahigh sensitivity and a fast response to NO_x gas at room temperature in air, leading to a low detection limit even down to 10 ppb, probably due to the synergic effects of the unique electronic conduction of black phosphorous and the heterostructure of the Co₃O₄ nanoparticles.

The inclusion of other processes, such as catalytic reactions and fluorescence quenching, often improves sensor capabilities through component nanoarchitectonics. Imanaka and co-workers used a combustion process induced by a precious-metal-free $\text{CeO}_2\text{-ZrO}_2\text{-ZnO}$ catalyst for CO gas detection [87]. The semiconducting (p-type) La_2CuO_4 -loaded $\text{CeO}_2\text{-ZrO}_2\text{-ZnO}$ catalyst has a small heat capacity and dramatically increases the temperature of the Pt coil, resulting in a highly sensitive sensor signal. On the other hand, the n-type Sm_2CuO_4 -loaded $\text{CeO}_2\text{-ZrO}_2\text{-ZnO}$ catalyst is advantageous when rapid response and low temperature operation are required. The selection of nanoarchitectonic component materials in sensing units can be used to optimize sensing performance according to usage.

Luminescent xerogel-based sensors for amine vapors were reported by Hanabusa and co-workers [88]. The xerogels used in this sensor system were prepared with fluorescent gelators containing a tris(β -diketonato) complex with appropriate metals. The presence of amines can be found through fluorescence-quenching efficiencies of the thin layer films of the gel materials. The prepared films are most sensitive to the detection of tertiary amines.

The discrimination and sensing of chiral substances are regarded as a more difficult task because chiral molecules have identical properties except for their optical activity. As recently reported by Kondo et al., the use of chiral receptors is the key to discriminate chiral substances [89]. They used tetraamide-based receptors having chiral L-serine and L-threonine to discriminate enantiomers of *N*-acetyl amino acid anions through ratiometric fluorescence analysis. Torsi and co-workers adopted odorant binding proteins to discriminate chiral substances [90]. They immobilized odorant binding proteins to the gate of a water-gated bio-organic transistor (Figure 3). In this construction, the source and drain patterned substrate was covered with p-type poly[2,5-bis(3-tetradecylthiophen-2-yl)thieno[3,2-b]thiophene], a water droplet and a Au-plate modified with the odorant binding protein as a gate. Enantiomers of odorant carvone could be clearly discriminated by this sensing system. The capacitance changes may be caused by the binding of the odorant to the protein accompanied with the derivation of the free-energy and conformational changes. Such capacitance-modulated transistors would be useful for molecular sensing with weak interaction and faint differences.

Kim and co-workers fabricated sensor arrays that were engineered with fluorescence dyes and cucurbit[*n*]urils ($n = 6, 7$ and 8) as host systems [91]. The obtained sensors were used for sensing biogenic amines with the aid of principal component analysis. This nanoarchitectonics strategy could be applied for



the sensing of various bio-related substances and may become useful for diagnostics of diseases such as cancer.

Sensors that are used to detect environmental risks mostly require detection of metal ions and toxic ions. Akamatsu et al. developed an optode-type sensor to visually detect cesium ions in domestic water and seawater [92] (Figure 4). The detection of radioactive cesium species becomes a serious demand after a nuclear plant explosion event, but radioactivity measurements do not always work with high areal resolution. The detection of cesium ions themselves with very high resolution would be useful together with radioactivity analysis. Cesium ion sensing using a film-type optode and nano-optode sensors would satisfy the former requirements. The optode sensors designed using nanoarchitectonic concepts incorporated a calix[6]arene derivative, responsive dye KD-M1337, and a cation exchanger sodium tetrakis[3,5-bis(trifluoromethyl)phenyl]borate. The binding of cesium ions to the calix[6]arene derivative shifts the equilibrium, resulting in color changes even in domestic water and seawater. Sonicating this optode mixture provides nano-optode sensor particles at a diameter of approximately 100 nm, which is a material capable of detection of cesium ions in sub-micromolar levels.

Use of 2D and layered materials in nanoarchitectonics for ion sensors is also investigated. Ruiz-Hitzky et al. reported the fabrication of potentiometric sensors for alkali-ion detection using clay materials intercalated with silacrown ethers, dimethylsila-14-crown-5 and dimethylsila-17-crown-6 [93]. The nanoengineered montmorillonite-based intercalation materials were included in poly(vinyl chloride)-based electrodes for potentiometric sensors towards alkali-metal ions in solution. Ultrasensitive sensors for mercury ions were prepared by Li et al. who engineered suspended atomically thin black phosphorus be-

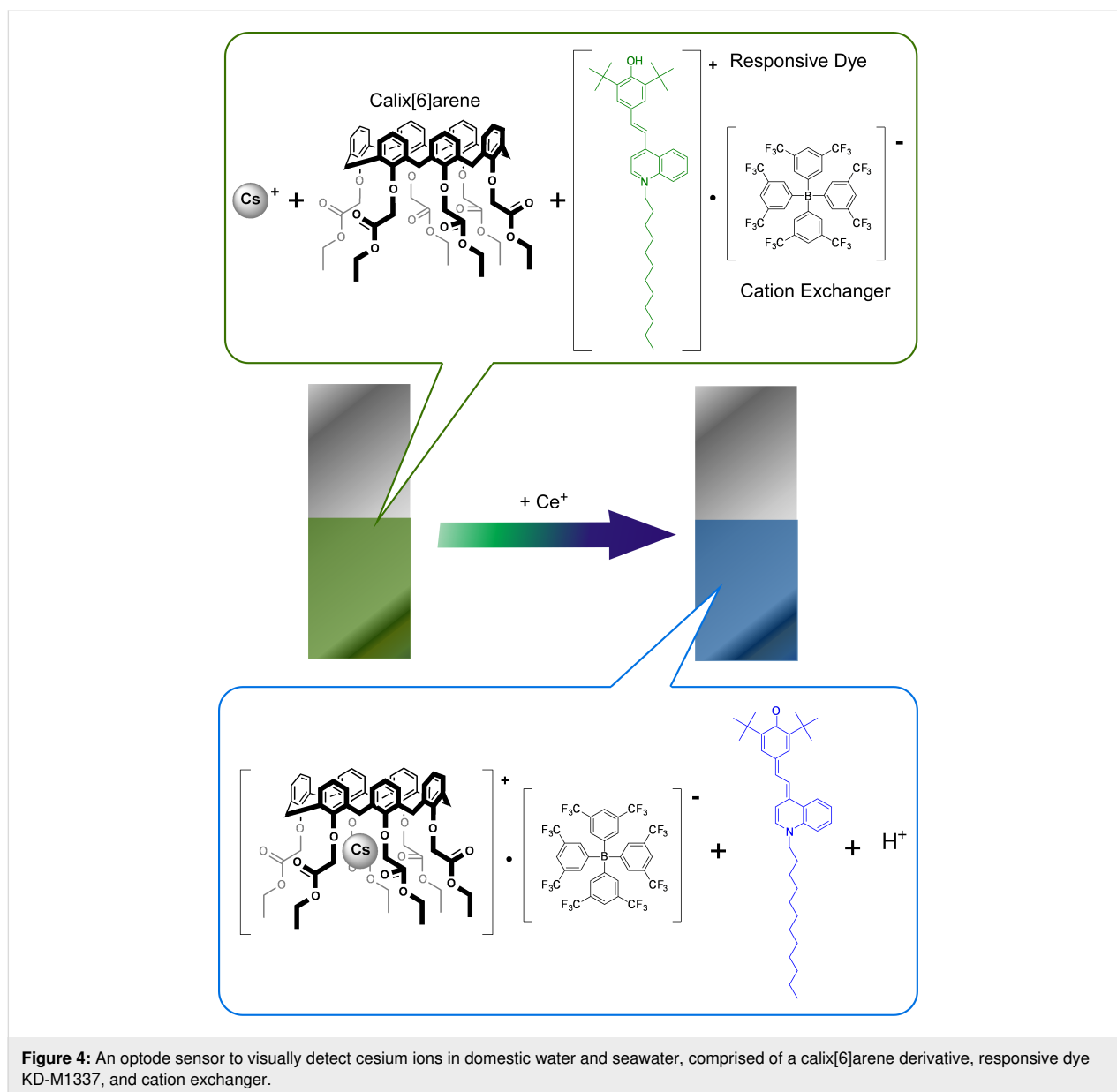


Figure 4: An optode sensor to visually detect cesium ions in domestic water and seawater, comprised of a calix[6]arene derivative, responsive dye KD-M1337, and cation exchanger.

tween the source and drain electrodes [94]. Due to the avoidance of substrate scattering, the sensors with bridged black phosphorus exhibit a much improved signal-to-noise ratio in mercury ion detection with a detection limit of 0.01 ppb and a very short detection time constant of 3 s. This nanoarchitectonic design can maximize the intrinsic potential of black phosphorus and other materials.

Sensors for physical conditions

Not limited to particular chemicals, the sensing of general external environments such as pH, humidity, pressure, and magnetic field is undoubtedly important. Spanu et al. reported sensitive pH sensors based on organic charge-modulated field-effect transistor structures with 6,13-bis(triisopropylsilyl)ethynyl-

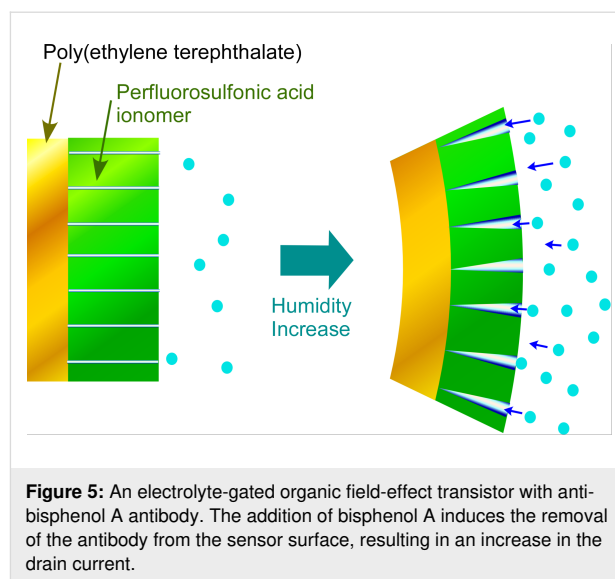
pentacene [95]. The fabricated sensors have a super-Nernstian sensitivity and reference-less nature. This organic charge-modulated field-effect transistor mechanism is attributed to the variation of the threshold voltage in the organic field-effect transistor induced by charge variation upon the presence of a charge (protonation, etc.) on the sensing area. The sensitivity of the nanoengineered sensors is easily tunable by adjusting geometry-related parameters.

For practical uses, sensors are not always used in ideal conditions. Especially, their use in dynamic human life, including health monitoring and medical applications, require consideration of bending and deformation according to typical human motions. Someya and co-workers developed transparent

bending-insensitive pressure sensors [96]. They nanoengineered pressure sensor materials from composites of carbon nanotubes and graphene with a fluorinated copolymer, vinylidene fluoride-tetrafluoroethylene-hexafluoropropylene, and an ionic liquid, 1-butyl-3-methylimidazolium bis(trifluoromethanesulphonyl)imide, through an electrospinning process. The prepared sensor can only sense normal pressure without significant disturbance up to a bending radius of 80 μm . This sensor system could be applicable for demands requiring the evaluation of small normal pressures even on dynamic surfaces such as natural tissues and is expected to be useful for in situ biomedical digital monitoring, such as palpation for breast cancer.

Triboelectric nanogenerators to convert mechanical energy to electricity have recently been given much attention as self-powered systems. These systems can be designed using nanoarchitectonic principles with various sensing materials to form energy harvesting self-powered sensors [97,98]. Chen and co-workers introduced a perfluorosulfonic acid ionomer as a water-vapor-driven actuation material for a triboelectric nanogenerator device to realize a highly sensitive humidity sensor [99] (Figure 5). The reaction of the sensing materials to humidity results in electrical changes for sensing. The perfluorosulfonic acid ionomer membrane has perpendicularly extended nanochannels that can adsorb moisture. Under relatively high humidity conditions, the adsorption of water molecules expands the nanochannels resulting in internal stress generation. These changes can be sensitively detected by the triboelectric nanogenerator. At the same time, the collection of such electrical signals can work as energy harvesting devices from wind and raindrops. Similarly, Liao, Wang, and co-workers used a triboelectric nanogenerator system of thin films of fluorinated ethylene propylene to fabricate self-powered wind sensors operating in free-standing mode (anemometer triboelectric nanogenerator) and single-electrode mode (wind vane triboelectric nanogenerator) [100]. The former mode can be used for analysis of wind speed with less energy consumption and the latter one provides an accurate measurement for the wind direction. The wireless monitoring of these responses could contribute to large-scale climate monitoring.

Although various living creatures, including bacteria, insects, birds, and sharks, can sense magnetic fields for orientation and navigation, humans are basically insensitive to magnetic fields. The human detection of magnetic fields can be realized using electro-skin-type sensors for magnetic fields. Makarov and co-workers developed giant magnetoresistive sensors in foil form having high flexibility and mechanical durability [101]. For giant magnetoresistive materials, multilayer structures of Co/Cu and permalloy/Cu multilayers (permalloy = $\text{Ni}_{81}\text{Fe}_{19}$)

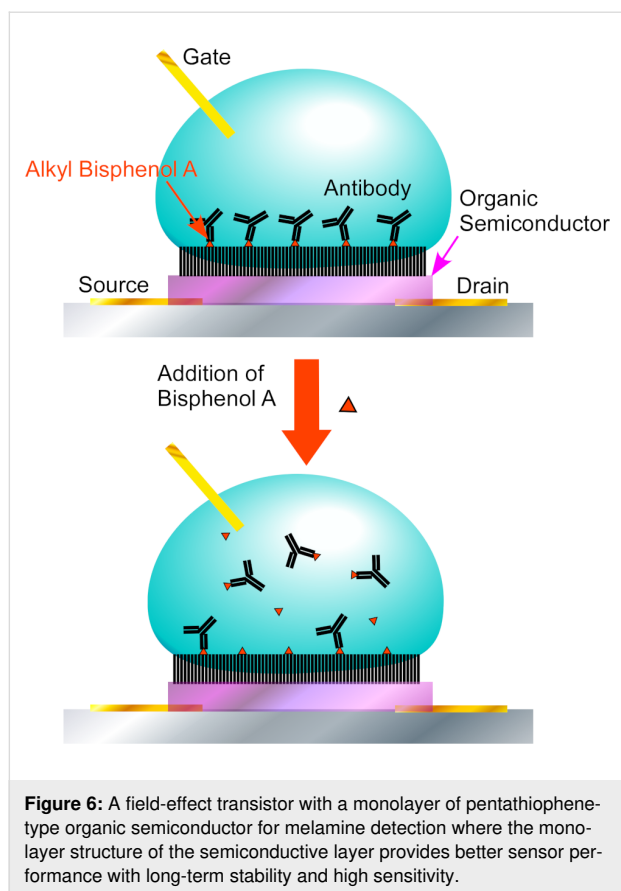


were engineered on ultrathin polyethylene terephthalate foils. The prepared sensors are extremely flexible (bending radii $<3 \mu\text{m}$) and light weight ($\approx 3 \text{ g m}^{-2}$). They are wearable and act as a magneto-sensitive skin with navigation and touchless control capabilities.

Biosensors

Because biosensors can provide crucial contributions to human life, medical, and health monitoring, the development of biosensors has received significant attention. For example, for the detection of bisphenol A, which is suspected as an endocrine disruptor, Piro et al. produced a nanoarchitectonic electrolyte-gated organic field-effect transistor with poly(2,5-bis(3-tetradecylthiophen-2-yl)thieno[3,2-b]thiophene) as an organic semiconductor co-crystallized with an alkyl derivative of bisphenol A as a haptent [102] (Figure 6). Upon binding of the anti-bisphenol A antibody, the output current of the transistor first decreased. The addition of bisphenol A induced the removal of the antibody from the sensor surface through competitive binding, resulting in a capacitance increase accompanied with an increase of the drain current. The switching-on signal response of this system is in the nM range of concentration threshold for bisphenol A detection. This sensitivity is sufficient for the detection and monitoring of this persistent pollutant in drinking water.

As mentioned previously, the discrimination of chiral substances is a rather tough goal in sensor design. However, the detection of chiral amino acids is an unavoidable matter in technologies related to protein metabolism, food products and pharmaceuticals. Such difficult goals can be achieved through a nanoarchitectonics approach, namely molecular imprinting [103-105]. Qiu and co-workers developed sensors for chirality



detection of amino acid guests using an organic electrochemical transistor with a poly(3,4-ethylenedioxythiophene)/poly(styrenesulfonate) (PEDOT/PSS) system modified with molecularly imprinted polymer films [106]. The selectivity factor of L-tryptophan over D-tryptophan and that of L-tyrosine over D-tyrosine were 11.6 and 14.5, respectively.

Life activities are also important targets in biosensor technology. Someya and co-workers developed a highly flexible organic amplifier to detect weak biosignals [107]. A highly conductive biocompatible gel composite made from multiwalled carbon nanotubes and aqueous hydrogel was integrated into a two-dimensional organic amplifier. The biocompatible nature of these nanoarchitectures is advantageous to favorably interface the bio-tissues and device electrodes. The dynamic motion of a living heart can be sensitively monitored without mechanical interference. This enables the direct evaluation of epicardial electrocardiogram signals with an amplification factor of 200. This idea can be expanded to various practical sensing demands such as temporal monitoring during medical surgery and long-term implantable monitoring. Ingebrandt and co-workers also reported biosensors to monitor electrophysiological activity of the cardiac cell line HL-1 [108]. The sensing system is based on organic electrochemical transistors with PEDOT/PSS materials

produced with a wafer-scale process, which is known to be useful for transducing and amplifying biological ionic signals.

In certain cases, device architectures and cell nanoarchitectures have to be well-matched for better sensor performance. Hsing and co-workers investigated the difference in sensing signals between tightly packed colorectal adenocarcinoma cells and leaky nasopharyngeal carcinoma cells using biosensors based on an organic electrochemical transistor [109]. The biosensor performance depends on the impedance of whole the system, including the transistor devices and monitored cells. Since cell packing affects the sensor signal, the optimum design of such cell sensors should be tuned according to cell packing. In order to evaluate the paracellular characteristics of tightly packed cells, a large-sized organic electrochemical transistor is advantageous. On the other hand, the high frequency related information of leaky cells can be effectively monitored by smaller organic electrochemical transistors.

Biosensors based on the electrical double layer gated AlGaN/GaN high electron mobility transistors were used to dynamically monitor changes in the transmembrane potential, as reported by Lee, Wang, and co-workers [110]. Here, circulating tumor cells of colorectal cancer together with cellular bioelectric signals were investigated. The proposed sensor design would also be useful for the rapid screening of diseases as a point-of-care diagnostic tool. Owens and co-workers developed organic field-effect transistor systems with PEDOT/PSS materials for the detection of lactate [111]. Enhanced lactate production was detected for cancer cells because of their promoted activity of glycolytic metabolism. These nanoengineered miniaturized biosensors would be useful for the continuous monitoring of tumor status in cancer patients.

Advancements in nanoarchitectonic motifs

In the previous sections, several examples of advanced sensor systems were reviewed according to sensing targets, chemical substances, physical conditions, and biological activities. The importance of a high degree of structural control (microscopic and nanoscopic levels) both for the sensing materials and the device structures can be found in most of the cases. Advanced sensors are certainly improved by application of nanoarchitectonics strategies. In the following sections, sensor designs are discussed on the basis of nanoarchitectonic structural motifs, such as nanoporous structures and extremely thin nanofilms as well as the highly enhanced molecular sensing capability at interfacial structures.

Porous structures

One of the most highly effective methods to improve the sensitivity of sensors is the enhancement of the surface (interfacial)

area for facile contact between the sensing target molecules and sensor device material. High surface area materials such as integrated structures and nanoporous materials can be obtained by molecular self-assembly [112–114] and template synthesis [115–119]. For example, various sensors with self-assembled fullerene materials and their carbonized materials as sensing structures were reported for aromatic gas vapors [120,121] and carbonized particles [122]. Mesoporous carbons were used for sensing of tannins in acidic aqueous environment with highly cooperative adsorption in the mesochannels [123]. The nanoarchitectonic construction of carbon nanocages with high surface mesoporous structures [124] was integrated with electrospun polymer fibers and resulted in a highly sensitive sensing material for aniline vapor [125]. Layer-by-layer structures of mesoporous carbon capsules can work as sensing membranes capable of selectively sensing through the doping of secondary sensing units [126].

As an emerging nanoporous material, metal–organic frameworks and porous coordination polymers have received much attention because of the various functional nanoporous structures that can be engineered through self-assembly from selected components [127–130]. Pan, Su, and co-workers fabricated metal–organic framework materials with microporous structure and switchable luminescence capability for sensitive water detection [131]. The metal–organic framework sensor was prepared from Zn and (5-(2-(5-fluoro-2-hydroxyphenyl)-4,5-bis(4-fluorophenyl)-1*H*-imidazol-1-yl)isophthalic acid) ligands, the latter of which shows a characteristic excited state intramolecular proton transfer. The adsorption of water molecules into the micropores induces interconversion between the hydrated and dehydrated phase, accompanied by the switching on and off of the excited state intramolecular proton transfer, resulting in sensitive switching between two-color photoluminescence. The sensing films consisting of paper and ZnO could realize a very sensitive water detection with a relative humidity of less than 1% and the detection of trace-level water of less than 0.05%. In addition, the interference from any small molecules other than water is also avoided. The precise nanoarchitectonic control of the structure results in high sensitivity and selectivity.

The nanoporous architectures of metal–organic frameworks can also serve as filters for molecular selection. Fan and co-workers prepared an electrical gas sensor for formaldehyde with high selectivity using the molecular sieving function of zeolitic imidazolate framework structures on ZnO nanorods [132]. Core–shell structures of zeolitic imidazolate frameworks and ZnO nanorods were prepared by direct growth of the framework on the ZnO nanorods. Limitation effects by the framework aperture provided improved selectivity for formaldehyde

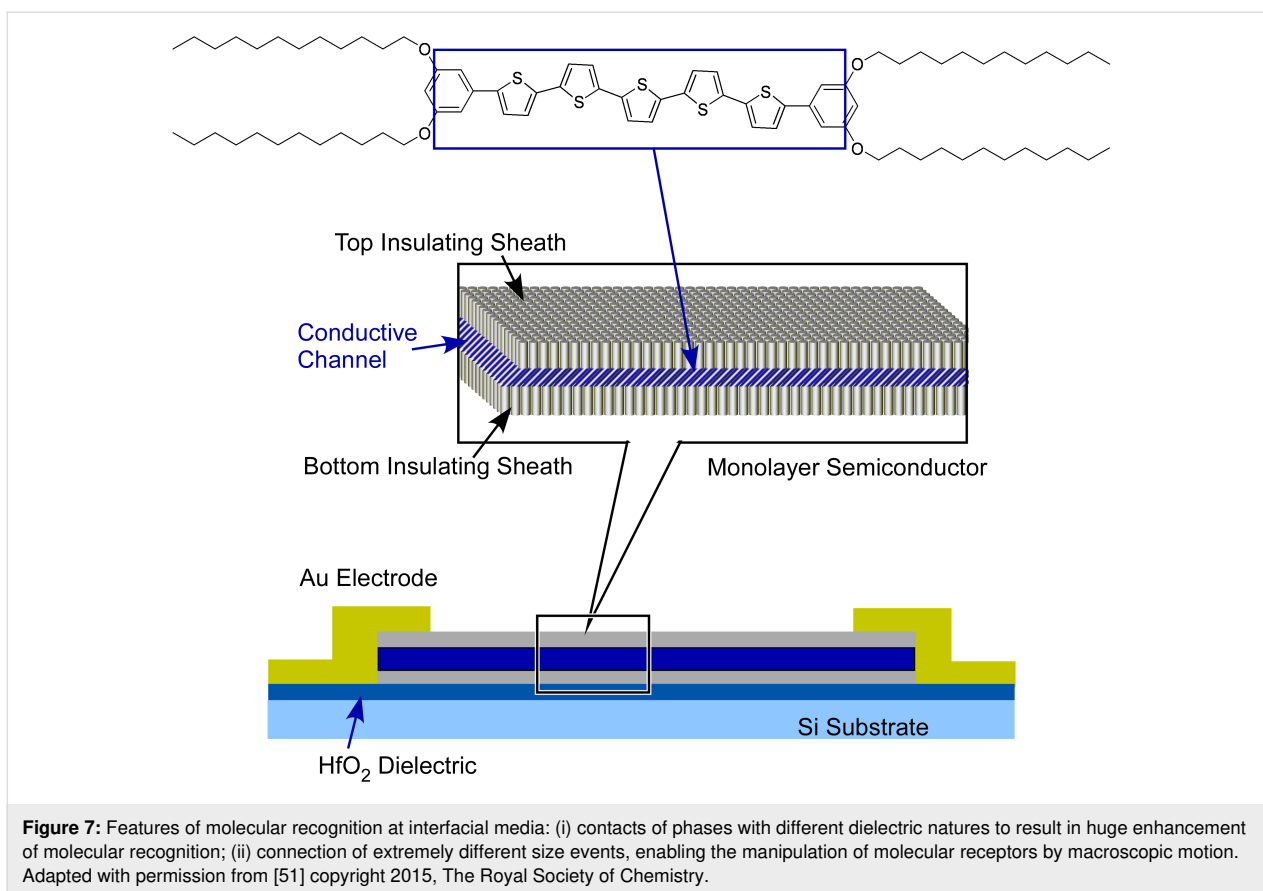
over the other volatile organic compounds. This nanoarchitectonic strategy using molecular sieving effects of nanoporous frameworks can be applied to other targets of selected molecular size.

Ultrathin films

The immobilization of functional materials with ultrathin films such as self-assembled monolayers [133,134], Langmuir–Blodgett films [135–137], and layer-by-layer assembly [138–141] on sensors and related devices is a key nanoarchitectonics step for sensor fabrication. For example, Furusawa et al. immobilized nickel-nitrilotriacetic acid within a self-assembled monolayer on an organic field-effect transistor, which was used for the sensitive detection of small organic acid molecules, such as citric acid [142]. Hattori and co-workers fabricated an ATP/ADP sensitive image sensor by immobilization of apyrase as a self-assembled monolayer on a 128×128 pixel array semiconductor CCD-type pH imaging sensor [143]. Although the sensitivity of the prepared sensor is inferior to that of other fluorescence sensors, this sensor nanoarchitectonics approach does not require any labelling procedures. Therefore, it may be useful for the estimation of ATP discharge in damaged cells.

Ultrathin film nanoarchitectures are crucial not only for the facile contact between analytes and the sensor device but also with respect to the carrier mobility for semiconductor-based sensor devices. The enhancement of sensor performance on ultrathin films has been recognized in several recent research efforts. Guo and co-workers fabricated a field-effect transistor with monolayers and multilayers of pentathiophene-type organic semiconductor for melamine detection [144] (Figure 7). The used dialkoxyphenyl pentathiophene derivative has a semiconductive pentathiophene core sandwiched by two insulating C_{12} alkyl chains. Long-range ordered π -conjugated columns in densely packed arrays of the pentathiophene core confine charge carrier transport to one direction. The charge generation and transport can be effectively maximized by this carrier transport confinement. The fabricated field-effect transistor structure was integrated into a microfluidic device. The monolayer structure of the semiconductive layer provided better sensor performance with long-term stability and high sensitivity. The minimum detection limit for melamine was approximately 10 ppb.

The high performance of nanoarchitectonic semiconductive monolayers was also demonstrated by Chan and co-workers who successfully prepared semiconductor monolayer crystals of 2,9-didecyldinaphtho[2,3-*b*:2',3'-*f*]thieno[3,2-*b*]thiophene on the millimeter scale [145]. The semiconductor crystals encapsulated within poly(methyl methacrylate) exhibited a significantly high mobility ($10.4 \text{ cm}^2 \text{ V}^{-1} \text{ s}^{-1}$). In multilayer structures,



the first layer on interface plays the main role in carrier transport and the layers above simply act as carrier suppliers. The crystal monolayer shows low anisotropy and thermally activated carrier transport. Such characteristics are different from the band-like carrier transport modes in thicker crystals. The fabricated sensor with ultrathin organic semiconductor crystals was an efficient NH_3 sensor with a detection limit on the 10 ppb level.

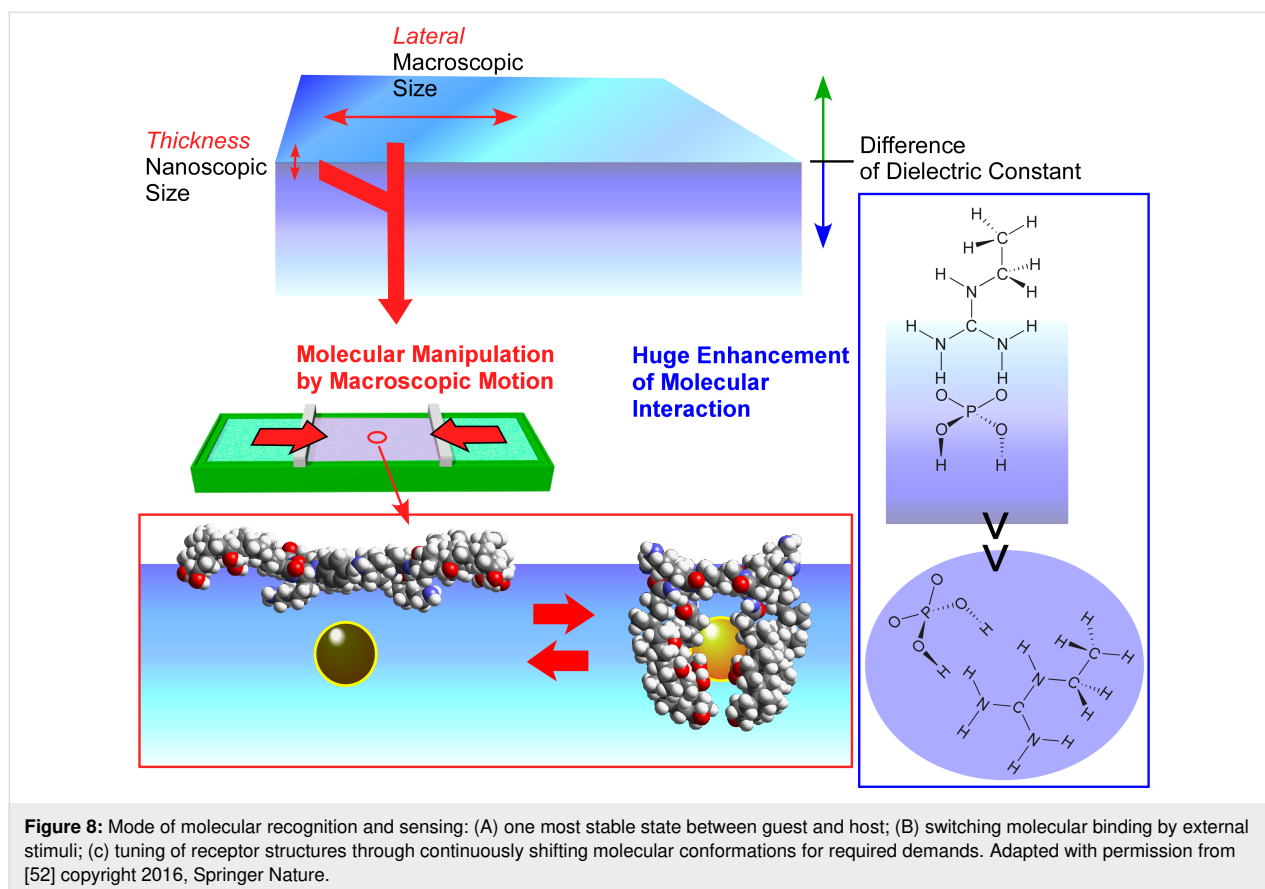
Specific effect of molecular sensing at interfaces

The high surface area nature of nanoporous materials and the ultrathin aspect of monolayer crystals are advantageous for improved sensor performance. These structural features can also be regarded as interfacial nanoarchitectonics. In this section, the scientific basis for molecular sensing (recognition and discrimination) specific to interfacial environments is briefly described and hints for future sensor designs are discussed. Interfacial environments provide two distinct features, (i) contacts of phases with different dielectric natures and (ii) connection of extremely different size events (both along the lateral direction and thickness direction, Figure 8).

Interfaces provide the potential of contact between two different media. Molecules with recognition capability (receptor mol-

ecules) prepared through organic synthesis are not always soluble in the aqueous phase and are not appropriate for sensing of water-soluble targets in solution phases. Placing such water-insoluble receptor molecules at a water-contacting interface is crucial to sense water-soluble substances such as important biomolecules. Not limited to this technical requirement, interfacial media have the benefit to greatly enhance molecular recognition capability [146,147].

Systematic research on the comparison of recognition efficiencies of a fixed molecular pair (guanidinium and phosphate) revealed that binding constants change significantly depending on interfacial types [148]. The binding constant between guanidinium and phosphate dispersed in aqueous media is only 1.4 M^{-1} [149]. This kind of molecular recognition based on hydrogen bonding and/or electrostatic interaction is weakened in polar media such as water phase. Chemical species with uneven charge distribution within a molecule are stabilized by solvation with polar solvent molecules, which is highly disadvantageous in the formation of host–guest complexes. However, the incorporation of guanidinium functionality into molecular assemblies such as aqueous micelles and lipid bilayers to place recognition sites at a mesoscopic interface increased the binding constants between guanidinium and phosphate to 10^2 – 10^4 M^{-1}



[148]. Furthermore, placing a guanidinium functionality at a macroscopic interface, such as air–water, results in a huge enhancement of the binding constant with aqueous phosphate to 10^6 – 10^7 M^{-1} [150,151]. These facts imply that the molecular sensing capability could be improved by selecting interfacial types and nanoarchitectonics of interfacial structures.

The above-mentioned specific features at the interfacial media were also proved by theoretical calculations based on quantum chemistry [152–154]. Even without direct contact, the low dielectric nature in nonpolar media located close to recognition sites provided positive effects. It is a plausible mechanism regarding how biological molecular recognition occurs in aqueous media [155]. The molecular recognition of small molecules can be accomplished at certain kind of interfacial environments such as cell membrane, inside surfaces of receptors and enzymes, and macromolecular interfaces at DNA and proteins. This mechanism for the enhancement of the molecular recognition capability at interfaces is surely applicable to other molecular recognition pairs and should also lead to highly efficient molecular recognition of various aqueous biomolecules including amino acids [156], peptides [157–159], sugars [160,161], nucleic acid bases [162,163], and nucleotides [164–166] at well-designed interfacial environments. In order to design and fabri-

cate sensors with better performance, interfacial nanoarchitectonics should be crucial factor.

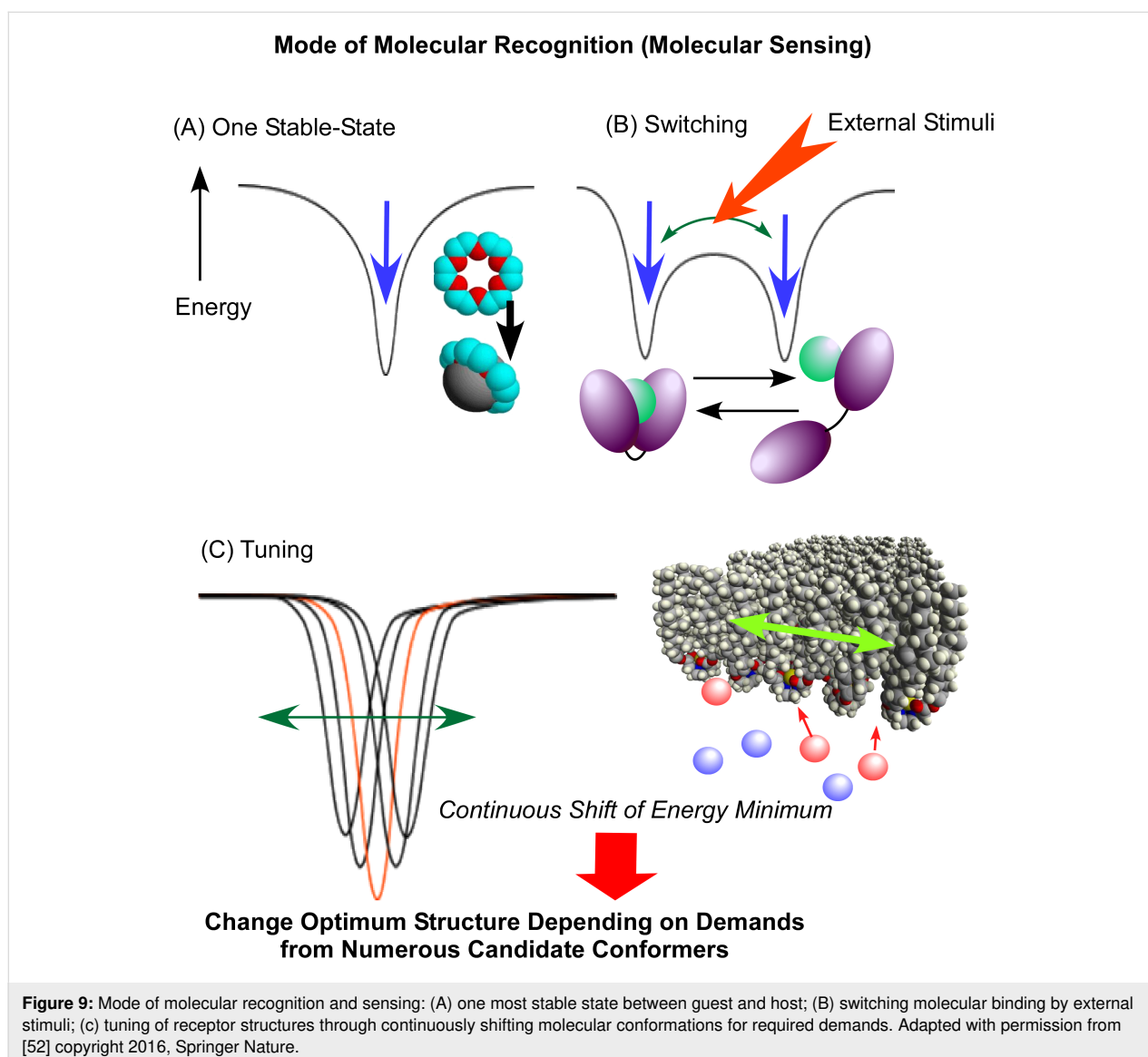
Another feature specific to interfacial environments is the co-existence of extremely different sized structures. At dynamic interfaces, their lateral direction has macroscopic motional freedom but the structural changes in the thickness direction are confined to the nanometer scale. Therefore, macroscopic motions such as compression and expansion can be coupled with nanoscopic conformational changes of molecules embedded at dynamic interfaces [167–169]. For example, dihedral angles of binaphthyl units can be continuously tuned at the molecular level by dynamic compression and expansion of monolayers of tens of centimeters [170]. The digital switching of helicity of binaphthyl units is also possible through macroscopic motion [171]. Furthermore, the control of nanoscopic motions of molecular machines such as molecular catchers [172,173] and molecular motors [174,175] can be accomplished by macroscopic motions at the air–water interface.

The regulation of molecular conformation at interfacial media can be utilized for the tuning of molecular sensing. The structural tuning of an octacoordinate Na^+ complex of a cholesterol-substituted cyclen with twisting helicity at the air–water inter-

face was used to realize switching recognition selectivity between L- and D-amino acids [176,177]. Chiral sensing can be tuned by mechanical deformation of the receptor membrane at the interfacial environment. Two-dimensional deformation of cholesterol-substituted triazacyclononane monolayer was used to optimize the discrimination between uracil and thymine derivatives [178,179] that cannot be discriminated by naturally occurring DNA and RNA. Although the structural difference between uracil and thymine is only one methyl group, the difference in the binding constant between them is more than 60 times. A mechanically controlled indicator displacement assay for aqueous glucose detection based on fluorescence resonance energy transfer was also reported [180].

The mechanisms of molecular recognition and sensing are roughly summarized in Figure 9. The most basic mechanism

(Figure 9) is considered to form the most stable state between the guest and host [181-183]. Shinkai and co-workers proposed a breakthrough approach to switch molecular recognition using photo-isomerization of an azobenzene moiety in a receptor structure (Figure 9) [184,185]. This mechanism creates two (or more) states with different binding energies that are controlled by external stimuli. This can also be regarded as the origination of molecular function control by external stimuli. It shares working principles with molecular machines which are usually operated by switching between several states [186-188]. Unlike these pioneering approaches, the mechanical tuning of receptor molecules at interfacial media considers numerous candidates from continuously shifting molecular conformations (Figure 9) [189-191]. This method may use all available possibilities of flexible molecular structures. This methodology has not been fully applied in practical sensing systems so far.



Conclusion

This review article introduces several examples of recent advanced sensors, classified according to the sensing targets (chemical substance, physical condition and biological phenomena) in the first part. In the second part, the importance of nanoarchitected motifs, such as nanoporous structures, ultrathin films, and unusual interfacial effects, for improved sensor performance is discussed. Most of the examples illustrate the crucial role of the nanostructure in sensor design. Although fine structural control used to be an important task in device miniaturization and integration in past approaches, the importance of precise nanoscale control for sensor materials is widely recognized in recent developments. Molecular sieving effects for better selectivity by well-designed nanoporous structures and effective carrier transport within a well-packed ultrathin monolayer of organic semiconductors have become clear in recent research examples. Of course, further efforts regarding nanoscale design of sensing materials for better performance and selectivity have to be made. In many cases, sensor advancements can be implemented with the nanoarchitectonics methodologies.

However, some important mechanisms such as huge enhancements of molecular recognition efficiency and molecular tuning capability at interfaces still remain as basic milestones and have not been applied in practical sensor applications to date. Further advancements of sensors can be made by exploitation of the various flexible and dynamic natures of sensing materials where various interactions and effects have to be harmonized similar to the nanoarchitectonics strategy. In addition, dynamic harmonization of the interactions is also commonly observed in biological processes and systems. As discussed in some reviews, interfacing between electronic devices and ionic biosystems [192] and biocompatible device design [193] are crucial for future sensor devices. Therefore, investigation on dynamic nanoarchitectonics for sensor devices could lead to further advancements in bio-friendly sensor devices.

Of course, all important sensor activities cannot be described in this review. For example, sensors based on various advanced physical mechanisms such as plasmonic [194], dielectric sensing [195], surface-enhanced Raman scattering [196], Fabry–Pérot-based intraocular pressure [197], and/or novel nanostructured materials with exotic properties [198] undoubtedly have important contributions. In addition, mass-sensitive sensors, quartz and crystal microbalance [199] are useful for many substances because mass changes and alteration of viscoelasticity such as phase transition [200] are common over all materials. Once developed, these technologies have to be translated into real-world applications for potential impact on daily life. A roadmap for this technology transfer cannot be

easily predicted, but should include important factors such as miniaturization, wearable features, scalability, reliability, and sampling of analytes. This roadmap would be shortened by using new types of materials such as two-dimensional materials [201–204] and through introducing new methodologies such as mass-data analyses and machine learning [205,206]. Another important factor to accelerate progress would be process integration of top down microfabrication and bottom up self-organization to bridge materials and systems over a wide scale range. To combine all of these techniques and functional materials, the concept of nanoarchitectonics becomes a crucial bridge in this roadmap.

Acknowledgements

This study was partially supported by JSPS KAKENHI Grant Number JP16H06518 (Coordination Asymmetry) and CREST JST Grant Number JPMJCR1665.

ORCID® iDs

Katsuhiko Ariga - <https://orcid.org/0000-0002-2445-2955>

Taizo Mori - <https://orcid.org/0000-0002-6974-5137>

Shun Watanabe - <https://orcid.org/0000-0001-7377-6043>

References

- Imran, M.; Motta, N.; Shafiei, M. *Beilstein J. Nanotechnol.* **2018**, *9*, 2128–2170. doi:10.3762/bjnano.9.202
- Zhang, Y.; Yuan, S.; Day, G.; Wang, X.; Yang, X.; Zhou, H.-C. *Coord. Chem. Rev.* **2018**, *354*, 28–45. doi:10.1016/j.ccr.2017.06.007
- Dey, A. *Mater. Sci. Eng., B* **2018**, *229*, 206–217. doi:10.1016/j.mseb.2017.12.036
- Sun, D.; Luo, Y.; Debliquy, M.; Zhang, C. *Beilstein J. Nanotechnol.* **2018**, *9*, 2832–2844. doi:10.3762/bjnano.9.264
- Datta, K. K. R.; Reddy, B. V. S.; Ariga, K.; Vinu, A. *Angew. Chem., Int. Ed.* **2010**, *49*, 5961–5965. doi:10.1002/anie.201001699
- Chaikittisilp, W.; Ariga, K.; Yamauchi, Y. *J. Mater. Chem. A* **2013**, *1*, 14–19. doi:10.1039/c2ta00278g
- Jeevanandam, J.; Barhoum, A.; Chan, Y. S.; Dufresne, A.; Danquah, M. K. *Beilstein J. Nanotechnol.* **2018**, *9*, 1050–1074. doi:10.3762/bjnano.9.98
- Irie, M.; Morimoto, M. *Bull. Chem. Soc. Jpn.* **2018**, *91*, 237–250. doi:10.1246/bcsj.20170365
- Ishihara, S.; Labuta, J.; Nakanishi, T.; Tanaka, T.; Kataura, H. *ACS Sens.* **2017**, *2*, 1405–1409. doi:10.1021/acssensors.7b00591
- Sarikhani, Z.; Manoochehri, M. *Bull. Chem. Soc. Jpn.* **2017**, *90*, 746–753. doi:10.1246/bcsj.20160407
- Rasheed, T.; Bilal, M.; Nabeel, F.; Iqbal, H. M. N.; Li, C.; Zhou, Y. *Sci. Total Environ.* **2018**, *615*, 476–485. doi:10.1016/j.scitotenv.2017.09.126
- Acharya, R.; Naik, B.; Parida, K. *Beilstein J. Nanotechnol.* **2018**, *9*, 1448–1470. doi:10.3762/bjnano.9.137
- Zhang, X.; Jia, S.; Song, J.; Wu, S.; Han, X. *Bull. Chem. Soc. Jpn.* **2018**, *91*, 998–1007. doi:10.1246/bcsj.20180014
- Shak, K. P. Y.; Pang, Y. L.; Mah, S. K. *Beilstein J. Nanotechnol.* **2018**, *9*, 2479–2498. doi:10.3762/bjnano.9.232

15. Hou, J.; Inganäs, O.; Friend, R. H.; Gao, F. *Nat. Mater.* **2018**, *17*, 119–128. doi:10.1038/nmat5063
16. Miyasaka, T. *Bull. Chem. Soc. Jpn.* **2018**, *91*, 1058–1068. doi:10.1246/bcsj.20180071
17. Guo, D.; Shibuya, R.; Akiba, C.; Saji, S.; Kondo, T.; Nakamura, J. *Science* **2016**, *351*, 361–365. doi:10.1126/science.aad0832
18. Chaikittisilp, W.; Hu, M.; Wang, H.; Huang, H.-S.; Fujita, T.; Wu, K. C.-W.; Chen, L.-C.; Yamauchi, Y.; Ariga, K. *Chem. Commun.* **2012**, *48*, 7259–7261. doi:10.1039/c2cc33433j
19. Watanabe, M.; Dokko, K.; Ueno, K.; Thomas, M. L. *Bull. Chem. Soc. Jpn.* **2018**, *91*, 1660–1682. doi:10.1246/bcsj.20180216
20. Kawai, T.; Nakao, S.; Nishide, H.; Oyaizu, K. *Bull. Chem. Soc. Jpn.* **2018**, *91*, 721–727. doi:10.1246/bcsj.20170420
21. Yamamura, A.; Watanabe, S.; Uno, M.; Mitani, M.; Mitsui, C.; Tsurumi, J.; Isahaya, N.; Kanaoka, Y.; Okamoto, T.; Takeya, J. *Sci. Adv.* **2018**, *4*, eaao5758. doi:10.1126/sciadv.aao5758
22. Ulaganathan, R. K.; Chang, Y.-H.; Wang, D.-Y.; Li, S.-S. *Bull. Chem. Soc. Jpn.* **2018**, *91*, 761–771. doi:10.1246/bcsj.20180016
23. Watanabe, Y.; Sasabe, H.; Kido, J. *Bull. Chem. Soc. Jpn.* **2019**, *92*, 716–728. doi:10.1246/bcsj.20180336
24. Ariga, K.; Lvov, Y. M.; Kawakami, K.; Ji, Q.; Hill, J. P. *Adv. Drug Delivery Rev.* **2011**, *63*, 762–771. doi:10.1016/j.addr.2011.03.016
25. Li, B. L.; Setyawati, M. I.; Chen, L.; Xie, J.; Ariga, K.; Lim, C.-T.; Garaj, S.; Leong, D. T. *ACS Appl. Mater. Interfaces* **2017**, *9*, 15286–15296. doi:10.1021/acsami.7b02529
26. He, H.; Xu, B. *Bull. Chem. Soc. Jpn.* **2018**, *91*, 900–906. doi:10.1246/bcsj.20180038
27. Kumar, J.; Liz-Marzán, L. M. *Bull. Chem. Soc. Jpn.* **2019**, *92*, 30–37. doi:10.1246/bcsj.20180236
28. Povie, G.; Segawa, Y.; Nishihara, T.; Miyauchi, Y.; Itami, K. *Science* **2017**, *356*, 172–175. doi:10.1126/science.aam8158
29. Sun, Z.; Matsuno, T.; Isobe, H. *Bull. Chem. Soc. Jpn.* **2018**, *91*, 907–921. doi:10.1246/bcsj.20180051
30. Sun, Z.; Ikemoto, K.; Fukunaga, T. M.; Koretsune, T.; Arita, R.; Sato, S.; Isobe, H. *Science* **2019**, *363*, 151–155. doi:10.1126/science.aau5441
31. Ruiz-Hitzky, E.; Darder, M.; Aranda, P.; Ariga, K. *Adv. Mater. (Weinheim, Ger.)* **2010**, *22*, 323–336. doi:10.1002/adma.200901134
32. Seiki, N.; Shoji, Y.; Kajitani, T.; Ishiwari, F.; Kosaka, A.; Hikima, T.; Takata, M.; Someya, T.; Fukushima, T. *Science* **2015**, *348*, 1122–1126. doi:10.1126/science.aab1391
33. Sawada, T.; Serizawa, T. *Bull. Chem. Soc. Jpn.* **2018**, *91*, 455–466. doi:10.1246/bcsj.20170428
34. Xing, R.; Yuan, C.; Li, S.; Song, J.; Li, J.; Yan, X. *Angew. Chem., Int. Ed.* **2018**, *57*, 1537–1542. doi:10.1002/anie.201710642
35. Dhiman, S.; George, S. J. *Bull. Chem. Soc. Jpn.* **2018**, *91*, 687–699. doi:10.1246/bcsj.20170433
36. Ringleb, F.; Andree, S.; Heidmann, B.; Bonse, J.; Eylers, K.; Ernst, O.; Boeck, T.; Schmid, M.; Krüger, J. *Beilstein J. Nanotechnol.* **2018**, *9*, 3025–3038. doi:10.3762/bjnano.9.281
37. Mori, T.; Tanaka, H.; Dalui, A.; Mitoma, N.; Suzuki, K.; Matsumoto, M.; Aggarwal, N.; Patnaik, A.; Acharya, S.; Shrestha, L. K.; Sakamoto, H.; Itami, K.; Ariga, K. *Angew. Chem., Int. Ed.* **2018**, *57*, 9679–9683. doi:10.1002/anie.201803859
38. Chen, R.; Kang, J.; Kang, M.; Lee, H.; Lee, H. *Bull. Chem. Soc. Jpn.* **2018**, *91*, 979–990. doi:10.1246/bcsj.20180042
39. Sung, B.; Kim, M.-H. *Beilstein J. Nanotechnol.* **2018**, *9*, 205–215. doi:10.3762/bjnano.9.22
40. Asanuma, H.; Murayama, K.; Kamiya, Y.; Kashida, H. *Bull. Chem. Soc. Jpn.* **2018**, *91*, 1739–1748. doi:10.1246/bcsj.20180278
41. Ariga, K.; Jia, X.; Song, J.; Hsieh, C.-T.; Hsu, S.-h. *ChemNanoMat* **2019**, *5*, 692–702. doi:10.1002/cnma.201900207
42. Einaga, Y. *Bull. Chem. Soc. Jpn.* **2018**, *91*, 1752–1762. doi:10.1246/bcsj.20180268
43. Kitamori, T. *Bull. Chem. Soc. Jpn.* **2019**, *92*, 469–473. doi:10.1246/bcsj.20180276
44. Xie, Y.; Ding, Y.; Li, X.; Wang, C.; Hill, J. P.; Ariga, K.; Zhang, W.; Zhu, W. *Chem. Commun.* **2012**, *48*, 11513–11515. doi:10.1039/c2cc36140j
45. Izawa, H.; Wada, M.; Nishino, S.; Sumita, M.; Fujita, T.; Morihashi, K.; Ifuku, S.; Morimoto, M.; Saimoto, H. *Bull. Chem. Soc. Jpn.* **2018**, *91*, 1220–1225. doi:10.1246/bcsj.20180128
46. Wang, Y.; Michinobu, T. *Bull. Chem. Soc. Jpn.* **2017**, *90*, 1388–1400. doi:10.1246/bcsj.20170294
47. Maduraiveeran, G.; Sasidharan, M.; Ganesan, V. *Biosens. Bioelectron.* **2018**, *103*, 113–129. doi:10.1016/j.bios.2017.12.031
48. Huang, R.; He, N.; Li, Z. *Biosens. Bioelectron.* **2018**, *109*, 27–34. doi:10.1016/j.bios.2018.02.053
49. Ferhan, A. R.; Jackman, J. A.; Park, J. H.; Cho, N.-J.; Kim, D.-H. *Adv. Drug Delivery Rev.* **2018**, *125*, 48–77. doi:10.1016/j.addr.2017.12.004
50. Li, B. L.; Wang, J.; Gao, Z. F.; Shi, H.; Zou, H. L.; Ariga, K.; Leong, D. T. *Mater. Horiz.* **2019**, *6*, 563–570. doi:10.1039/c8mh01232f
51. Ariga, K.; Ji, Q.; Nakanishi, W.; Hill, J. P.; Aono, M. *Mater. Horiz.* **2015**, *2*, 406–413. doi:10.1039/c5mh00012b
52. Ariga, K.; Minami, K.; Ebara, M.; Nakanishi, J. *Polym. J.* **2016**, *48*, 371–389. doi:10.1038/pj.2016.8
53. Ishihara, S.; Labuta, J.; Van Rossom, W.; Ishikawa, D.; Minami, K.; Hill, J. P.; Ariga, K. *Phys. Chem. Chem. Phys.* **2014**, *16*, 9713–9746. doi:10.1039/c3cp55431g
54. Ariga, K.; Ji, Q.; Hill, J. P.; Bando, Y.; Aono, M. *NPG Asia Mater.* **2012**, *4*, e17. doi:10.1038/am.2012.30
55. Ariga, K.; Nishikawa, M.; Mori, T.; Takeya, J.; Shrestha, L. K.; Hill, J. P. *Sci. Technol. Adv. Mater.* **2019**, *20*, 51–95. doi:10.1080/14686996.2018.1553108
56. Ariga, K.; Li, M.; Richards, G. J.; Hill, J. P. *J. Nanosci. Nanotechnol.* **2011**, *11*, 1–13. doi:10.1166/jnn.2011.3839
57. Ariga, K.; Li, J.; Fei, J.; Ji, Q.; Hill, J. P. *Adv. Mater. (Weinheim, Ger.)* **2016**, *28*, 1251–1286. doi:10.1002/adma.201502545
58. Ramanathan, M.; Shrestha, L. K.; Mori, T.; Ji, Q.; Hill, J. P.; Ariga, K. *Phys. Chem. Chem. Phys.* **2013**, *15*, 10580–10611. doi:10.1039/c3cp50620g
59. Nakanishi, W.; Minami, K.; Shrestha, L. K.; Ji, Q.; Hill, J. P.; Ariga, K. *Nano Today* **2014**, *9*, 378–394. doi:10.1016/j.nantod.2014.05.002
60. Ariga, K.; Malgras, V.; Ji, Q.; Zakaria, M. B.; Yamauchi, Y. *Coord. Chem. Rev.* **2016**, *320–321*, 139–152. doi:10.1016/j.ccr.2016.01.015
61. Sakakibara, K.; Hill, J. P.; Ariga, K. *Small* **2011**, *7*, 1288–1308. doi:10.1002/smll.201002350
62. Ariga, K.; Vinu, A.; Yamauchi, Y.; Ji, Q.; Hill, J. P. *Bull. Chem. Soc. Jpn.* **2012**, *85*, 1–32. doi:10.1246/bcsj.20110162
63. Ariga, K.; Yamauchi, Y.; Rydzek, G.; Ji, Q.; Yonamine, Y.; Wu, K. C.-W.; Hill, J. P. *Chem. Lett.* **2014**, *43*, 36–68. doi:10.1246/cl.130987

64. Ariga, K.; Watanabe, S.; Mori, T.; Takeya, J. *NPG Asia Mater.* **2018**, *10*, 90–106. doi:10.1038/s41427-018-0022-9
65. Sang, Y.; Liu, M. *Mol. Syst. Des. Eng.* **2019**, *4*, 11–28. doi:10.1039/c8me00068a
66. Abe, H.; Liu, J.; Ariga, K. *Mater. Today* **2016**, *19*, 12–18. doi:10.1016/j.mattod.2015.08.021
67. Ariga, K.; Ishihara, S.; Abe, H. *CrystEngComm* **2016**, *18*, 6770–6778. doi:10.1039/c6ce00986g
68. Kim, J.; Kim, J. H.; Ariga, K. *Joule* **2017**, *1*, 739–768. doi:10.1016/j.joule.2017.08.018
69. Khan, A. H.; Ghosh, S.; Pradhan, B.; Dalui, A.; Shrestha, L. K.; Acharya, S.; Ariga, K. *Bull. Chem. Soc. Jpn.* **2017**, *90*, 627–648. doi:10.1246/bcsj.20170043
70. Ariga, K.; Yamauchi, Y.; Ji, Q.; Yonamine, Y.; Hill, J. P. *APL Mater.* **2014**, *2*, 030701. doi:10.1063/1.4868177
71. Pandeewar, M.; Senanayak, S. P.; Govindaraju, T. *ACS Appl. Mater. Interfaces* **2016**, *8*, 30362–30371. doi:10.1021/acsami.6b10527
72. Ariga, K.; Ji, Q.; McShane, M. J.; Lvov, Y. M.; Vinu, A.; Hill, J. P. *Chem. Mater.* **2012**, *24*, 728–737. doi:10.1021/cm202281m
73. Ariga, K.; Ji, Q.; Mori, T.; Naito, M.; Yamauchi, Y.; Abe, H.; Hill, J. P. *Chem. Soc. Rev.* **2013**, *42*, 6322–6345. doi:10.1039/c2cs35475f
74. Komiyama, M.; Yoshimoto, K.; Sisido, M.; Ariga, K. *Bull. Chem. Soc. Jpn.* **2017**, *90*, 967–1004. doi:10.1246/bcsj.20170156
75. Ariga, K.; Leong, D. T.; Mori, T. *Adv. Funct. Mater.* **2018**, *28*, 1702905. doi:10.1002/adfm.201702905
76. Ariga, K.; Kawakami, K.; Ebara, M.; Kotsuchibashi, Y.; Ji, Q.; Hill, J. P. *New J. Chem.* **2014**, *38*, 5149–5163. doi:10.1039/c4nj00864b
77. Pandey, A. P.; Girase, N. M.; Patil, M. D.; Patil, P. O.; Patil, D. A.; Deshmukh, P. K. *J. Nanosci. Nanotechnol.* **2014**, *14*, 828–840. doi:10.1166/jnn.2014.9014
78. Zhao, L.; Zou, Q.; Yan, X. *Bull. Chem. Soc. Jpn.* **2019**, *92*, 70–79. doi:10.1246/bcsj.20180248
79. Ariga, K.; Minami, K.; Shrestha, L. K. *Analyst* **2016**, *141*, 2629–2638. doi:10.1039/c6an00057f
80. Jackman, J. A.; Cho, N.-J.; Nishikawa, M.; Yoshikawa, G.; Mori, T.; Shrestha, L. K.; Ariga, K. *Chem. – Asian J.* **2018**, *13*, 3366–3377. doi:10.1002/asia.201800935
81. Aono, M.; Ariga, K. *Adv. Mater. (Weinheim, Ger.)* **2016**, *28*, 989–992. doi:10.1002/adma.201502868
82. Ariga, K. *Mater. Chem. Front.* **2017**, *1*, 208–211. doi:10.1039/c6qm00240d
83. Osica, I.; Imamura, G.; Shiba, K.; Ji, Q.; Shrestha, L. K.; Hill, J. P.; Kurzydowski, K. J.; Yoshikawa, G.; Ariga, K. *ACS Appl. Mater. Interfaces* **2017**, *9*, 9945–9954. doi:10.1021/acsami.6b15680
84. Osica, I.; Melo, A. F. A. A.; Imamura, G.; Shiba, K.; Ji, Q.; Hill, J. P.; Crespihlo, F. N.; Kurzydowski, K. J.; Yoshikawa, G.; Ariga, K. *J. Nanosci. Nanotechnol.* **2017**, *17*, 5908–5917. doi:10.1166/jnn.2017.14388
85. Tang, K.; Song, Z.; Tang, Q.; Tian, H.; Tong, Y.; Liu, Y. *IEEE Electron Device Lett.* **2018**, *39*, 119–122. doi:10.1109/led.2017.2770181
86. Liu, Y.; Wang, Y.; Ikram, M.; Lv, H.; Chang, J.; Li, Z.; Ma, L.; Rehman, A. U.; Lu, G.; Chen, J.; Shi, K. *ACS Sens.* **2018**, *3*, 1576–1583. doi:10.1021/acssensors.8b00397
87. Rodlamul, P.; Tamura, S.; Imanaka, N. *Bull. Chem. Soc. Jpn.* **2019**, *92*, 585–591. doi:10.1246/bcsj.20180284
88. Sasaki, J.; Suzuki, M.; Hanabusa, K. *Bull. Chem. Soc. Jpn.* **2018**, *91*, 538–547. doi:10.1246/bcsj.20170409
89. Kondo, S.-i.; Sato, K.; Matsuta, Y.; Osawa, K. *Bull. Chem. Soc. Jpn.* **2018**, *91*, 875–881. doi:10.1246/bcsj.20180028
90. Mulla, M. Y.; Tuccori, E.; Magliulo, M.; Lattanzi, G.; Palazzo, G.; Persaud, K.; Torsi, L. *Nat. Commun.* **2015**, *6*, 6010. doi:10.1038/ncomms7010
91. Park, K. M.; Kim, J.; Ko, Y. H.; Ahn, Y.; Murray, J.; Li, M.; Shrinidhi, A.; Kim, K. *Bull. Chem. Soc. Jpn.* **2018**, *91*, 95–99. doi:10.1246/bcsj.20170302
92. Akamatsu, M.; Komatsu, H.; Matsuda, A.; Mori, T.; Nakanishi, W.; Sakai, H.; Hill, J. P.; Ariga, K. *Bull. Chem. Soc. Jpn.* **2017**, *90*, 678–683. doi:10.1246/bcsj.20170046
93. Ruiz-Hitzky, E.; Gómez-Avilés, A.; Darder, M.; Aranda, P. *Bull. Chem. Soc. Jpn.* **2018**, *91*, 608–616. doi:10.1246/bcsj.20170425
94. Li, P.; Zhang, D.; Jiang, C.; Zong, X.; Cao, Y. *Biosens. Bioelectron.* **2017**, *98*, 68–75. doi:10.1016/j.bios.2017.06.027
95. Spanu, A.; Viola, F.; Lai, S.; Cosseddu, P.; Ricci, P. C.; Bonfiglio, A. *Org. Electron.* **2017**, *48*, 188–193. doi:10.1016/j.orgel.2017.06.010
96. Lee, S.; Reuveny, A.; Reeder, J.; Lee, S.; Jin, H.; Liu, Q.; Yokota, T.; Sekitani, T.; Isoyama, T.; Abe, Y.; Suo, Z.; Someya, T. *Nat. Nanotechnol.* **2016**, *11*, 472–478. doi:10.1038/nnano.2015.324
97. Cao, R.; Pu, X.; Du, X.; Yang, W.; Wang, J.; Guo, H.; Zhao, S.; Yuan, Z.; Zhang, C.; Li, C.; Wang, Z. L. *ACS Nano* **2018**, *12*, 5190–5196. doi:10.1021/acsnano.8b02477
98. Askari, H.; Hashemi, E.; Khajepour, A.; Khamesee, M. B.; Wang, Z. L. *Nano Energy* **2018**, *53*, 1003–1019. doi:10.1016/j.nanoen.2018.09.032
99. Ren, Z.; Ding, Y.; Nie, J.; Wang, F.; Xu, L.; Lin, S.; Chen, X.; Wang, Z. L. *ACS Appl. Mater. Interfaces* **2019**, *11*, 6143–6153. doi:10.1021/acsami.8b21477
100. Wang, J.; Ding, W.; Pan, L.; Wu, C.; Yu, H.; Yang, L.; Liao, R.; Wang, Z. L. *ACS Nano* **2018**, *12*, 3954–3963. doi:10.1021/acsnano.8b01532
101. Melzer, M.; Kaltenbrunner, M.; Makarov, D.; Karnaushenko, D.; Karnaushenko, D.; Sekitani, T.; Someya, T.; Schmidt, O. G. *Nat. Commun.* **2015**, *6*, 6080. doi:10.1038/ncomms7080
102. Piro, B.; Wang, D.; Benaoudia, D.; Tibaldi, A.; Anquetin, G.; Noël, V.; Reisberg, S.; Mattana, G.; Jackson, B. *Biosens. Bioelectron.* **2017**, *92*, 215–220. doi:10.1016/j.bios.2017.02.020
103. Komiyama, M.; Mori, T.; Ariga, K. *Bull. Chem. Soc. Jpn.* **2018**, *91*, 1075–1111. doi:10.1246/bcsj.20180084
104. Lai, Y.; Deng, Y.; Yang, G.; Li, S.; Zhang, C.; Liu, X. *J. Biomed. Nanotechnol.* **2018**, *14*, 1688–1694. doi:10.1166/jbn.2018.2617
105. Takeuchi, T.; Sunayama, H. *Chem. Commun.* **2018**, *54*, 6243–6251. doi:10.1039/c8cc02923g
106. Zhang, L.; Wang, G.; Xiong, C.; Zheng, L.; He, J.; Ding, Y.; Lu, H.; Zhang, G.; Cho, K.; Qiu, L. *Biosens. Bioelectron.* **2018**, *105*, 121–128. doi:10.1016/j.bios.2018.01.035
107. Sekitani, T.; Yokota, T.; Kuribara, K.; Kaltenbrunner, M.; Fukushima, T.; Inoue, Y.; Sekino, M.; Isoyama, T.; Abe, Y.; Onodera, H.; Someya, T. *Nat. Commun.* **2016**, *7*, 11425. doi:10.1038/ncomms11425
108. Hempel, F.; Law, J. K.-Y.; Nguyen, T. C.; Munief, W.; Lu, X.; Pachauri, V.; Susloparova, A.; Vu, X. T.; Ingebrandt, S. *Biosens. Bioelectron.* **2017**, *93*, 132–138. doi:10.1016/j.bios.2016.09.047

109. Yeung, S. Y.; Gu, X.; Tsang, C. M.; Tsao, S. W.; Hsing, I.-m. *Sens. Actuators, A* **2019**, *287*, 185–193. doi:10.1016/j.sna.2018.12.032
110. Pulikkathodi, A. K.; Sarangadharan, I.; Chen, Y.-H.; Lee, G.-Y.; Chyi, J.-I.; Lee, G.-B.; Wang, Y.-L. *Lab Chip* **2018**, *18*, 1047–1056. doi:10.1039/c7lc01305a
111. Braendlein, M.; Pappa, A.-M.; Ferro, M.; Lopresti, A.; Acquaviva, C.; Mamessier, E.; Malliaras, G. G.; Owens, R. M. *Adv. Mater. (Weinheim, Ger.)* **2017**, *29*, 1605744. doi:10.1002/adma.201605744
112. Cherumukkil, S.; Vedhanarayanan, B.; Das, G.; Praveen, V. K.; Ajayaghosh, A. *Bull. Chem. Soc. Jpn.* **2018**, *91*, 100–120. doi:10.1246/bcsj.20170334
113. Shimizu, T. *Bull. Chem. Soc. Jpn.* **2018**, *91*, 623–668. doi:10.1246/bcsj.20170424
114. Liu, X.; Riess, J. G.; Krafft, M. P. *Bull. Chem. Soc. Jpn.* **2018**, *91*, 846–857. doi:10.1246/bcsj.20170431
115. Hu, M.; Reboul, J.; Furukawa, S.; Torad, N. L.; Ji, Q.; Srinivasu, P.; Ariga, K.; Kitagawa, S.; Yamauchi, Y. *J. Am. Chem. Soc.* **2012**, *134*, 2864–2867. doi:10.1021/ja208940u
116. Chaikkittisilp, W.; Torad, N. L.; Li, C.; Imura, M.; Suzuki, N.; Ishihara, S.; Ariga, K.; Yamauchi, Y. *Chem. – Eur. J.* **2014**, *20*, 4217–4221. doi:10.1002/chem.201304404
117. Malgras, V.; Ji, Q.; Kamachi, Y.; Mori, T.; Shieh, F.-K.; Wu, K. C.-W.; Ariga, K.; Yamauchi, Y. *Bull. Chem. Soc. Jpn.* **2015**, *88*, 1171–1200. doi:10.1246/bcsj.20150143
118. Saptiama, I.; Kaneti, Y. V.; Oveisi, H.; Suzuki, Y.; Tsuchiya, K.; Takai, K.; Sakae, T.; Pradhan, S.; Hossain, M. S. A.; Fukumitsu, N.; Ariga, K.; Yamauchi, Y. *Bull. Chem. Soc. Jpn.* **2018**, *91*, 195–200. doi:10.1246/bcsj.20170295
119. Sai-Anand, G.; Sivanesan, A.; Benzigar, M. R.; Singh, G.; Gopalan, A.-I.; Baskar, A. V.; Ilbeygi, H.; Ramadass, K.; Kambala, V.; Vinu, A. *Bull. Chem. Soc. Jpn.* **2019**, *92*, 216–244. doi:10.1246/bcsj.20180280
120. Shrestha, L. K.; Shrestha, R. G.; Yamauchi, Y.; Hill, J. P.; Nishimura, T.; Miyazawa, K.; Kawai, T.; Okada, S.; Wakabayashi, K.; Ariga, K. *Angew. Chem., Int. Ed.* **2015**, *54*, 951–955. doi:10.1002/anie.201408856
121. Bairi, P.; Minami, K.; Nakanishi, W.; Hill, J. P.; Ariga, K.; Shrestha, L. K. *ACS Nano* **2016**, *10*, 6631–6637. doi:10.1021/acsnano.6b01544
122. Bairi, P.; Minami, K.; Hill, J. P.; Ariga, K.; Shrestha, L. K. *ACS Nano* **2017**, *11*, 7790–7796. doi:10.1021/acsnano.7b01569
123. Ariga, K.; Vinu, A.; Ji, Q.; Ohmori, O.; Hill, J. P.; Acharya, S.; Koike, J.; Shiratori, S. *Angew. Chem., Int. Ed.* **2008**, *47*, 7254–7257. doi:10.1002/anie.200802820
124. Ariga, K.; Vinu, A.; Miyahara, M.; Hill, J. P.; Mori, T. *J. Am. Chem. Soc.* **2007**, *129*, 11022–11023. doi:10.1021/ja074870t
125. Kosaki, Y.; Izawa, H.; Ishihara, S.; Kawakami, K.; Sumita, M.; Tateyama, Y.; Ji, Q.; Krishnan, V.; Hishita, S.; Yamauchi, Y.; Hill, J. P.; Vinu, A.; Shiratori, S.; Ariga, K. *ACS Appl. Mater. Interfaces* **2013**, *5*, 2930–2934. doi:10.1021/am400940q
126. Ji, Q.; Yoon, S. B.; Hill, J. P.; Vinu, A.; Yu, J.-S.; Ariga, K. *J. Am. Chem. Soc.* **2009**, *131*, 4220–4221. doi:10.1021/ja9010354
127. Torad, N. L.; Hu, M.; Ishihara, S.; Sukegawa, H.; Belik, A. A.; Imura, M.; Ariga, K.; Sakka, Y.; Yamauchi, Y. *Small* **2014**, *10*, 2096–2107. doi:10.1002/sml.201302910
128. Mei, L.; Shi, W.-q.; Chai, Z.-f. *Bull. Chem. Soc. Jpn.* **2018**, *91*, 554–562. doi:10.1246/bcsj.20170418
129. Li, J.; Wang, X.; Zhao, G.; Chen, C.; Chai, Z.; Alsaedi, A.; Hayat, T.; Wang, X. *Chem. Soc. Rev.* **2018**, *47*, 2322–2356. doi:10.1039/c7cs00543a
130. Azhar, A.; Li, Y.; Cai, Z.; Zakaria, M. B.; Masud, M. K.; Hossain, M. S. A.; Kim, J.; Zhang, W.; Na, J.; Yamauchi, Y.; Hu, M. *Bull. Chem. Soc. Jpn.* **2019**, *92*, 875–904. doi:10.1246/bcsj.20180368
131. Chen, L.; Ye, J.-W.; Wang, H.-P.; Pan, M.; Yin, S.-Y.; Wei, Z.-W.; Zhang, L.-Y.; Wu, K.; Fan, Y.-N.; Su, C.-Y. *Nat. Commun.* **2017**, *8*, 15985. doi:10.1038/ncomms15985
132. Tian, H.; Fan, H.; Li, M.; Ma, L. *ACS Sens.* **2016**, *1*, 243–250. doi:10.1021/acssensors.5b00236
133. Takimiya, K.; Nakano, M. *Bull. Chem. Soc. Jpn.* **2018**, *91*, 121–140. doi:10.1246/bcsj.20170298
134. Suda, M. *Bull. Chem. Soc. Jpn.* **2018**, *91*, 19–28. doi:10.1246/bcsj.20170283
135. Ariga, K.; Yamauchi, Y.; Mori, T.; Hill, J. P. *Adv. Mater. (Weinheim, Ger.)* **2013**, *25*, 6477–6512. doi:10.1002/adma.201302283
136. Seki, T. *Bull. Chem. Soc. Jpn.* **2018**, *91*, 1026–1057. doi:10.1246/bcsj.20180076
137. Ariga, K.; Mori, T.; Li, J. *Langmuir* **2019**, *35*, 3585–3599. doi:10.1021/acs.langmuir.8b01434
138. Ji, Q.; Honma, I.; Paek, S.-M.; Akada, M.; Hill, J. P.; Vinu, A.; Ariga, K. *Angew. Chem., Int. Ed.* **2010**, *49*, 9737–9739. doi:10.1002/anie.201004929
139. Rydzek, G.; Ji, Q.; Li, M.; Schaaf, P.; Hill, J. P.; Boulmedais, F.; Ariga, K. *Nano Today* **2015**, *10*, 138–167. doi:10.1016/j.nantod.2015.02.008
140. Ji, Q.; Qiao, X.; Liu, X.; Jia, H.; Yu, J.-S.; Ariga, K. *Bull. Chem. Soc. Jpn.* **2018**, *91*, 391–397. doi:10.1246/bcsj.20170357
141. Rodrigues, V. C.; Moraes, M. L.; Soares, J. C.; Soares, A. C.; Sanfelice, R.; Deffune, E.; Oliveira, O. N., Jr. *Bull. Chem. Soc. Jpn.* **2018**, *91*, 891–896. doi:10.1246/bcsj.20180019
142. Furusawa, H.; Ichimura, Y.; Harada, S.; Uematsu, M.; Xue, S.; Nagamine, K.; Tokito, S. *Bull. Chem. Soc. Jpn.* **2018**, *91*, 1020–1025. doi:10.1246/bcsj.20180065
143. Endo, S.; Kato, R.; Sawada, K.; Hattori, T. *Bull. Chem. Soc. Jpn.* **2018**, *91*, 304–310. doi:10.1246/bcsj.20170304
144. Chen, H.; Dong, S.; Bai, M.; Cheng, N.; Wang, H.; Li, M.; Du, H.; Hu, S.; Yang, Y.; Yang, T.; Zhang, F.; Gu, L.; Meng, S.; Hou, S.; Guo, X. *Adv. Mater. (Weinheim, Ger.)* **2015**, *27*, 2113–2120. doi:10.1002/adma.201405378
145. Peng, B.; Huang, S.; Zhou, Z.; Chan, P. K. L. *Adv. Funct. Mater.* **2017**, *27*, 1700999. doi:10.1002/adfm.201700999
146. Ariga, K.; Kunitake, T. *Acc. Chem. Res.* **1998**, *31*, 371–378. doi:10.1021/ar970014i
147. Ariga, K.; Ito, H.; Hill, J. P.; Tsukube, H. *Chem. Soc. Rev.* **2012**, *41*, 5800–5835. doi:10.1039/c2cs35162e
148. Onda, M.; Yoshihara, K.; Koyano, H.; Ariga, K.; Kunitake, T. *J. Am. Chem. Soc.* **1996**, *118*, 8524–8530. doi:10.1021/ja960991+
149. Springs, B.; Haake, P. *Bioorg. Chem.* **1977**, *6*, 181–190. doi:10.1016/0045-2068(77)90019-0
150. Sasaki, D. Y.; Kurihara, K.; Kunitake, T. *J. Am. Chem. Soc.* **1991**, *113*, 9685–9686. doi:10.1021/ja00025a051
151. Sasaki, D. Y.; Kurihara, K.; Kunitake, T. *J. Am. Chem. Soc.* **1992**, *114*, 10994–10995. doi:10.1021/ja00053a065
152. Sakurai, M.; Tamagawa, H.; Furuki, T.; Inoue, Y.; Ariga, K.; Kunitake, T. *Chem. Lett.* **1995**, *24*, 1001–1002. doi:10.1246/cl.1995.1001

153. Sakurai, M.; Tamagawa, H.; Inoue, Y.; Ariga, K.; Kunitake, T. *J. Phys. Chem. B* **1997**, *101*, 4810–4816. doi:10.1021/jp9700591
154. Tamagawa, H.; Sakurai, M.; Inoue, Y.; Ariga, K.; Kunitake, T. *J. Phys. Chem. B* **1997**, *101*, 4817–4825. doi:10.1021/jp9700600
155. Ariga, K. *ChemNanoMat* **2016**, *2*, 333–343. doi:10.1002/cnma.201600053
156. Ikeura, Y.; Kurihara, K.; Kunitake, T. *J. Am. Chem. Soc.* **1991**, *113*, 7342–7350. doi:10.1021/ja00019a035
157. Cha, X.; Ariga, K.; Onda, M.; Kunitake, T. *J. Am. Chem. Soc.* **1995**, *117*, 11833–11838. doi:10.1021/ja00153a003
158. Cha, X.; Ariga, K.; Kunitake, T. *J. Am. Chem. Soc.* **1996**, *118*, 9545–9551. doi:10.1021/ja961526f
159. Ariga, K.; Kamino, A.; Cha, X.; Kunitake, T. *Langmuir* **1999**, *15*, 3875–3885. doi:10.1021/la981047p
160. Kurihara, K.; Ohto, K.; Tanaka, Y.; Aoyama, Y.; Kunitake, T. *J. Am. Chem. Soc.* **1991**, *113*, 444–450. doi:10.1021/ja00002a010
161. Ariga, K.; Isoyama, K.; Hayashida, O.; Aoyama, Y.; Okahata, Y. *Chem. Lett.* **1998**, *27*, 1007–1008. doi:10.1246/cl.1998.1007
162. Kurihara, K.; Ohto, K.; Honda, Y.; Kunitake, T. *J. Am. Chem. Soc.* **1991**, *113*, 5077–5079. doi:10.1021/ja00013a063
163. Kawahara, T.; Kurihara, K.; Kunitake, T. *Chem. Lett.* **1992**, *21*, 1839–1842. doi:10.1246/cl.1992.1839
164. Taguchi, K.; Ariga, K.; Kunitake, T. *Chem. Lett.* **1995**, *24*, 701–702. doi:10.1246/cl.1995.701
165. Ariga, K.; Kamino, A.; Koyano, H.; Kunitake, T. *J. Mater. Chem.* **1997**, *7*, 1155–1161. doi:10.1039/a700081b
166. Oishi, Y.; Torii, Y.; Kato, T.; Kuramori, M.; Suehiro, K.; Ariga, K.; Taguchi, K.; Kamino, A.; Koyano, H.; Kunitake, T. *Langmuir* **1997**, *13*, 519–524. doi:10.1021/la960112x
167. Ariga, K.; Mori, T.; Hill, J. P. *Adv. Mater. (Weinheim, Ger.)* **2012**, *24*, 158–176. doi:10.1002/adma.201102617
168. Ariga, K.; Mori, T.; Ishihara, S.; Kawakami, K.; Hill, J. P. *Chem. Mater.* **2014**, *26*, 519–532. doi:10.1021/cm401999f
169. Ariga, K.; Mori, T.; Nakanishi, W.; Hill, J. P. *Phys. Chem. Chem. Phys.* **2017**, *19*, 23658–23676. doi:10.1039/c7cp02280h
170. Ishikawa, D.; Mori, T.; Yonamine, Y.; Nakanishi, W.; Cheung, D. L.; Hill, J. P.; Ariga, K. *Angew. Chem., Int. Ed.* **2015**, *54*, 8988–8991. doi:10.1002/anie.201503363
171. Mori, T.; Ishikawa, D.; Yonamine, Y.; Fujii, Y.; Hill, J. P.; Ichinose, I.; Ariga, K.; Nakanishi, W. *ChemPhysChem* **2017**, *18*, 1470–1474. doi:10.1002/cphc.201601144
172. Ariga, K.; Terasaka, Y.; Sakai, D.; Tsuji, H.; Kikuchi, J.-i. *J. Am. Chem. Soc.* **2000**, *122*, 7835–7836. doi:10.1021/ja000924m
173. Ariga, K.; Nakanishi, T.; Terasaka, Y.; Tsuji, H.; Sakai, D.; Kikuchi, J.-i. *Langmuir* **2005**, *21*, 976–981. doi:10.1021/la0477845
174. Mori, T.; Komatsu, H.; Sakamoto, N.; Suzuki, K.; Hill, J. P.; Matsumoto, M.; Sakai, H.; Ariga, K.; Nakanishi, W. *Phys. Chem. Chem. Phys.* **2018**, *20*, 3073–3078. doi:10.1039/c7cp04256f
175. Mori, T.; Chin, H.; Kawashima, K.; Ngo, H. T.; Cho, N.-J.; Nakanishi, W.; Hill, J. P.; Ariga, K. *ACS Nano* **2019**, *13*, 2410–2419. doi:10.1021/acsnano.8b09320
176. Michinobu, T.; Shinoda, S.; Nakanishi, T.; Hill, J. P.; Fujii, K.; Player, T. N.; Tsukube, H.; Ariga, K. *J. Am. Chem. Soc.* **2006**, *128*, 14478–14479. doi:10.1021/ja066429t
177. Michinobu, T.; Shinoda, S.; Nakanishi, T.; Hill, J. P.; Fujii, K.; Player, T. N.; Tsukube, H.; Ariga, K. *Phys. Chem. Chem. Phys.* **2011**, *13*, 4895–4900. doi:10.1039/c0cp01990a
178. Mori, T.; Okamoto, K.; Endo, H.; Hill, J. P.; Shinoda, S.; Matsukura, M.; Tsukube, H.; Suzuki, Y.; Kanekiyo, Y.; Ariga, K. *J. Am. Chem. Soc.* **2010**, *132*, 12868–12870. doi:10.1021/ja106653a
179. Mori, T.; Okamoto, K.; Endo, H.; Sakakibara, K.; Hill, J. P.; Shinoda, S.; Matsukura, M.; Tsukube, H.; Suzuki, Y.; Kanekiyo, Y.; Ariga, K. *Nanoscale Res. Lett.* **2011**, *6*, 304. doi:10.1186/1556-276x-6-304
180. Sakakibara, K.; Joyce, L. A.; Mori, T.; Fujisawa, T.; Shabbir, S. H.; Hill, J. P.; Anslyn, E. V.; Ariga, K. *Angew. Chem., Int. Ed.* **2012**, *51*, 9643–9646. doi:10.1002/anie.201203402
181. Lehn, J.-M. *Angew. Chem., Int. Ed. Engl.* **1988**, *27*, 89–112. doi:10.1002/anie.198800891
182. Pedersen, C. J. *Angew. Chem., Int. Ed. Engl.* **1988**, *27*, 1021–1027. doi:10.1002/anie.198810211
183. Cram, D. J. *Angew. Chem., Int. Ed. Engl.* **1988**, *27*, 1009–1020. doi:10.1002/anie.198810093
184. Shinkai, S.; Manabe, O. *Top. Curr. Chem.* **1984**, *121*, 67–104. doi:10.1007/3-540-12821-2_3
185. Shinkai, S.; Ikeda, M.; Sugasaki, A.; Takeuchi, M. *Acc. Chem. Res.* **2001**, *34*, 494–503. doi:10.1021/ar000177y
186. Feringa, B. L. *Angew. Chem., Int. Ed.* **2017**, *56*, 11060–11078. doi:10.1002/anie.201702979
187. Sauvage, J.-P. *Angew. Chem., Int. Ed.* **2017**, *56*, 11080–11093. doi:10.1002/anie.201702992
188. Stoddart, J. F. *Angew. Chem., Int. Ed.* **2017**, *56*, 11094–11125. doi:10.1002/anie.201703216
189. Ariga, K. *Anal. Sci.* **2016**, *32*, 1141–1149. doi:10.2116/analsci.32.1141
190. Shirai, Y.; Minami, K.; Nakanishi, W.; Yonamine, Y.; Joachim, C.; Ariga, K. *Jpn. J. Appl. Phys.* **2016**, *55*, 1102A2. doi:10.7567/jjap.55.1102a2
191. Shrestha, L. K.; Mori, T.; Ariga, K. *Curr. Opin. Colloid Interface Sci.* **2018**, *35*, 68–80. doi:10.1016/j.cocis.2018.01.007
192. Nishizawa, M. *Bull. Chem. Soc. Jpn.* **2018**, *91*, 1141–1149. doi:10.1246/bcsj.20180064
193. Stauss, S.; Honma, I. *Bull. Chem. Soc. Jpn.* **2018**, *91*, 492–505. doi:10.1246/bcsj.20170325
194. Anker, J. N.; Hall, W. P.; Lyandres, O.; Shah, N. C.; Zhao, J.; Van Duyne, R. P. *Nat. Mater.* **2008**, *7*, 442–453. doi:10.1038/nmat2162
195. Tittel, A.; Leitis, A.; Liu, M.; Yesilkoy, F.; Choi, D.-Y.; Neshev, D. N.; Kivshar, Y. S.; Altug, H. *Science* **2018**, *360*, 1105–1109. doi:10.1126/science.aas9768
196. Vo-Dinh, T. *Sens. Actuators, B* **1995**, *29*, 183–189. doi:10.1016/0925-4005(95)01681-3
197. Narasimhan, V.; Siddique, R. H.; Lee, J. O.; Kumar, S.; Ndjamen, B.; Du, J.; Hong, N.; Sretavan, D.; Choo, H. *Nat. Nanotechnol.* **2018**, *13*, 512–519. doi:10.1038/s41565-018-0111-5
198. Sreekanth, K. V.; Alapan, Y.; Elkabbash, M.; Ilker, E.; Hinczewski, M.; Gurkan, U. A.; De Luca, A.; Strangi, G. *Nat. Mater.* **2016**, *15*, 621–627. doi:10.1038/nmat4609
199. Emir Diltemiz, S.; Keçilli, R.; Ersöz, A.; Say, R. *Sensors* **2017**, *17*, 454. doi:10.3390/s17030454
200. Okahata, Y.; Kimura, K.; Ariga, K. *J. Am. Chem. Soc.* **1989**, *111*, 9190–9194. doi:10.1021/ja00208a009
201. Tan, S. M.; Poh, H. L.; Sofer, Z.; Pumera, M. *Analyst* **2013**, *138*, 4885. doi:10.1039/c3an00535f
202. Marvan, P.; Mazánek, V.; Sofer, Z. *Nanoscale* **2019**, *11*, 4310–4317. doi:10.1039/c8nr09294j

203. Kang, J.; Wells, S. A.; Sangwan, V. K.; Lam, D.; Liu, X.; Luxa, J.; Sofer, Z.; Hersam, M. C. *Adv. Mater. (Weinheim, Ger.)* **2018**, *30*, 1802990. doi:10.1002/adma.201802990
204. Lee, C. M.; Jin, C. H.; Ahn, C. H.; Cho, H. K.; Lim, J. H.; Hwang, S. M.; Joo, J. *Bull. Chem. Soc. Jpn.* **2019**, *92*, 1094–1099. doi:10.1246/bcsj.20190004
205. Liakos, K.; Busato, P.; Moshou, D.; Pearson, S.; Bochtis, D. *Sensors* **2018**, *18*, 2674. doi:10.3390/s18082674
206. Fonollosa, J.; Solórzano, A.; Marco, S. *Sensors* **2018**, *18*, 553. doi:10.3390/s18020553

License and Terms

This is an Open Access article under the terms of the Creative Commons Attribution License (<http://creativecommons.org/licenses/by/4.0>). Please note that the reuse, redistribution and reproduction in particular requires that the authors and source are credited.

The license is subject to the *Beilstein Journal of Nanotechnology* terms and conditions: (<https://www.beilstein-journals.org/bjnano>)

The definitive version of this article is the electronic one which can be found at:
[doi:10.3762/bjnano.10.198](https://doi.org/10.3762/bjnano.10.198)